DTU Library

Partially recrystallized microstructures of cold-rolled copper and mechanical properties

Lin, Fengxiang; Delannay, Laurent; Zhang, Yubin; Pantleon, Wolfgang; Juul Jensen, Dorte

Published in:
Proceedings of the Risø International Symposium on Materials Science

Publication date:
2014

Document Version
Peer reviewed version

PARTIALLY RECRYSTALLIZED MICROSTRUCTURES OF COLD-ROLLED COPPER AND MECHANICAL PROPERTIES

F.X. Lin[*], L. Delannay[**], Y.B. Zhang[*], W. Pantleon[***],
D. Juul Jensen[*]

[*]Danish-Chinese Center for Nanometals, Section for Materials Science and Advanced Characterization, Department of Wind Energy, Technical University of Denmark, Risø Campus, 4000 Roskilde, Denmark
[**]Université Catholique de Louvain, iMMC, 4 Av. Georges Lemaître, 1348 Louvain-La-Neuve, Belgium
[***]Department of Mechanical Engineering, Section for Materials and Surface Engineering, Technical University of Denmark, 2800 Kongens Lyngby, Denmark

ABSTRACT

Creating a partially recrystallized microstructure by annealing is a possible strategy to increase the ductility of a heavily deformed metal. In this work, cold-rolled copper was used as a model material to investigate the effect of partial recrystallization on mechanical properties. The microstructural evolution and recrystallization kinetics during isothermal annealing were investigated by electron backscatter diffraction. The mechanical properties of the partially recrystallized samples were measured by tensile testing. For understanding the dependence of the mechanical properties on the recrystallized volume fraction, an analytical model was applied, which assumes that deformation is uniform throughout the polycrystalline aggregate. The modelling and experimental results are compared, and applications and limits of the model are discussed.

1. INTRODUCTION

Improving ductility of nanostructured and ultrafine-grained metals/alloys produced by plastic deformation is typically required for practical usage. A possible strategy is to anneal the as-deformed sample and to get a partially recrystallized microstructure. With the introduction of recrystallized grains, the strength of the sample decreases, but the work hardening ability of the recrystallized part may improve the ductility and formability of the material. Many experimental investigations applying this strategy have been reported (e.g. Jin and Lloyd 2004; Li, Zhang, Tao and Lu 2008; Ray, Hutchinson and Ghosh 2011). However, the observed dependency between the mechanical properties and the recrystallized volume fraction V_V shows great variations. The objective of this work is therefore in detail to characterize and quantify structural changes taking place during annealing in pure copper (99.95%) deformed to a high strain (ε_{vM}=2.7). Based on that, changes in microstructure and mechanical properties are correlated.

2. EXPERIMENTAL DETAILS

An oxygen free high conductivity copper (purity 99.95%) with an initial grain size of 72 µm (measured by the line intercept method ignoring twin boundaries) was used. A plate 20 mm thick, 50 mm wide and 100 mm long was cut and rolled at room temperature to a thickness reduction of 90%, corresponding to a von Mises strain of 2.7.

Specimens were cut from the rolled plate and annealed at 230 °C from 600 s to 14400 s. Microstructure and texture of the annealed specimens were characterized by electron backscatter diffraction (EBSD) in the longitudinal section using a step size of 1 µm. Recrystallized grains were determined from EBSD data using an in-house program called DRG (Wu and Juul Jensen 2008) based on three criteria: 1) the internal misorientations within a recrystallized grain is less than 1.5°; 2) the equivalent circular diameter of the grain is larger than 3 µm; 3) the grain is at least partially surrounded by high angle boundaries (HABs, with misorientations >15°). V_V was determined as the area fraction of all recrystallized grains in a longitudinal section.

Dogbone-shaped tensile specimens were cut from the rolled plate, with the tensile direction parallel to the rolling direction (RD). The gauge section was 10 mm long, 5 mm wide and 2 mm thick. The specimens were annealed at 230 °C for various durations to obtain structures with a controlled V_V. The engineering strain stress curves of the as-deformed and the partially recrystallized specimens were measured by uniaxial tensile tests at an initial strain rate of 1.6×10^{-3} s^{-1} at room temperature. The yield strength s_y was determined as the engineering stress corresponding to 0.2% elongation, while the uniform elongation e_u and ultimate tensile strength s_u were determined as the engineering strain and stress corresponding to the maximum load, respectively.

3. RESULTS

<u>3.1 Microstructural evolution during annealing.</u> Fig. 1 shows the microstructure at an initial stage of recrystallization. The deformed matrix (unrecrystallized part) is composed of bands of different orientations. Localized shear bands (LSBs) are observed at +/- 35° to RD, and are most often observed inside bands of copper/S orientations (purple and blue bands in Fig. 1a). Whether the LSBs are at positive or negative angles to RD is orientation dependent (Wagner, Engler and Lücke 1995); inside each band, LSBs are parallel to each other. The recrystallized grains tend to cluster in bands parallel to RD. This clustering tendency is determined by the deformed microstructure. In Fig. 1, two types of preferential nucleation sites seem to dominate: boundaries between two bands of different orientations and LSBs. Nucleation at a boundary between two bands leads to a string of recrystallized grains, aligned parallel to RD, whereas grains nucleated at LSBs are aligned with the LSBs (+/- 35° to RD) locally, but are also clustered along RD on a larger scale.

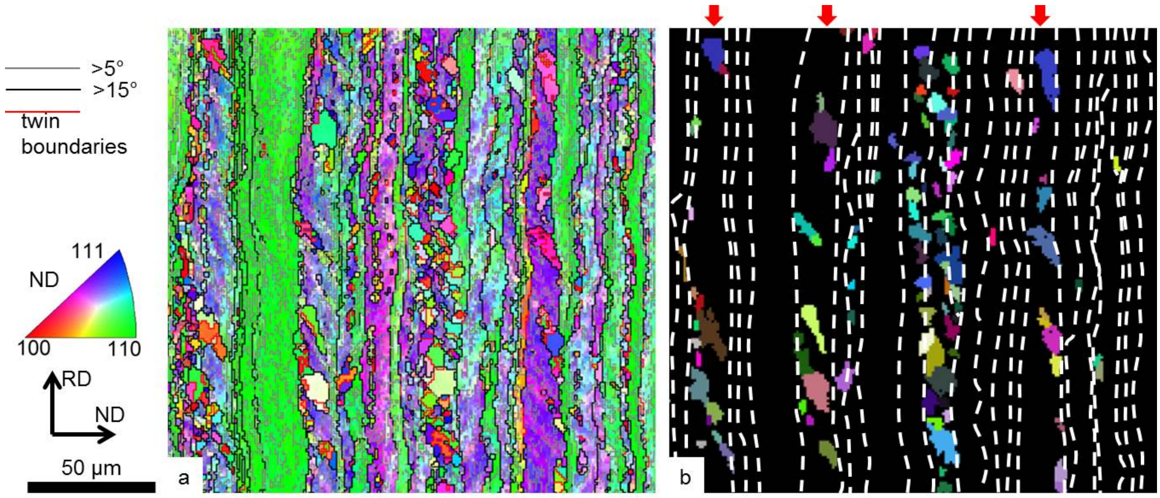

Fig. 1 Microstructure after 600 s annealing at 230 °C. a) Orientation map. b) Same map as a) with recrystallized grains highlighted in random colors and the unrecrystallized matrix in black. A grain and its twins are shown in the same color. Boundaries between two bands of different orientations in the matrix are outlined by white dashed lines to illustrate their relation with the locations of the recrystallized grains. The red arrows mark typical bands where nucleation from localized shear bands (LSBs) is observed.

As recrystallization continues, the recrystallized grains impinge upon each other along RD, whereas impingement along the normal direction (ND) is less significant (see Fig. 2). The impinged recrystallized grains begin to form complete bands parallel to RD, leading to a lamellar structure. The texture of the recrystallized part is weak, which is different from the strong cube texture observed in some cold-rolled and annealed copper (e.g. Ridha and Hutchinson 1982). The weak cube texture in this material is related to the relatively large initial grain size (Lin, Pantleon, Leffers and Juul Jensen 2012). Textural effects are therefore not considered in the following analysis.

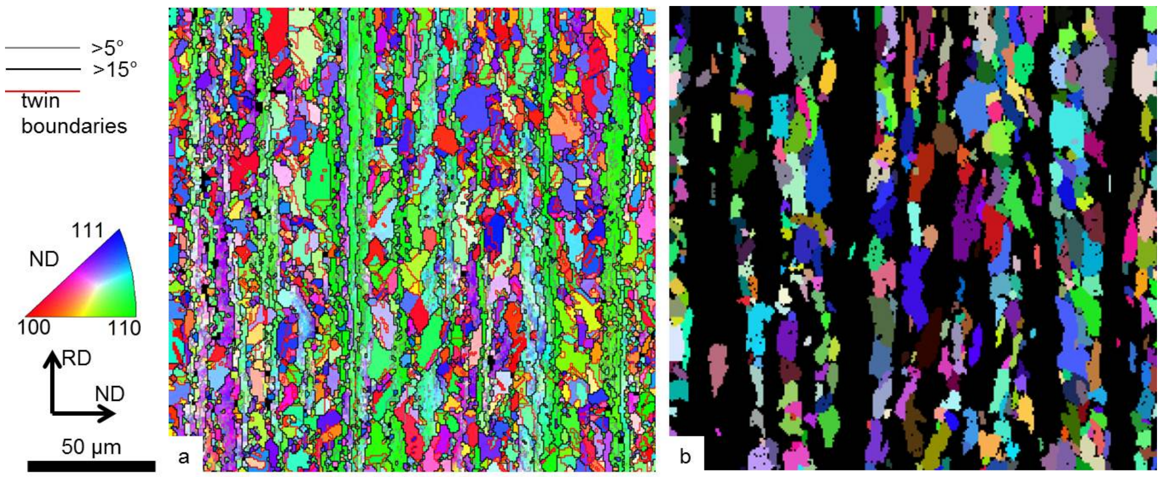

Fig. 2 Microstructure after 1800 s annealing at 230 °C. a) Orientation map. b) Same map as a) with recrystallized grains highlighted in random colors. A grain and its twins are shown in the same color.

<u>3.2 Recrystallization kinetics.</u> The increase of V_V with increasing annealing time t is usually described by the JMAK equation (Kolmogorov 1937, Johnson and Mehl 1939, Avrami 1939):

$$V_V = 1 - \exp(-kt^n) \quad (1)$$

Where k and n are constants. According to this equation, the data may be plotted in an "Avrami plot": $-ln(1\text{-}V_V)$ as a function of t on a log-log scale. The experimental data points fit roughly to a straight line (see Fig. 3a), which suggests that the JMAK equation describes the kinetics data well. But the slope, which corresponds to the exponent n in Eq. 1 is less than the theoretical value of 3 or 4. The clustered spatial distribution of the recrystallized grains, as described in Section 3.1, is one reason contributing to this low value of n (Lin, Zhang, Tao, Pantleon, Juul Jensen 2014).

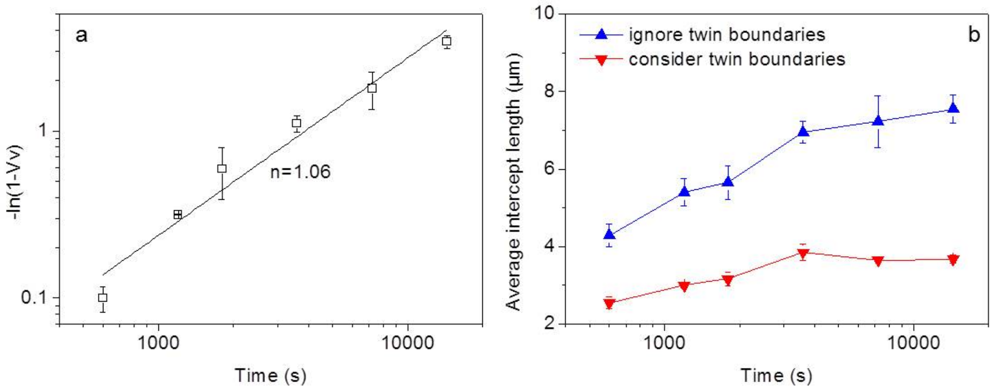

Fig. 3 Evolution of $–ln(1\text{-}V_V)$ (a) and average intercept length of recrystallized grains (b) as a function of annealing time t during isothermal annealing at 230 °C.

Fig. 3b shows the evolution of average grain size as a function of time t. The grain size was measured by the line intercept method. Twin boundaries were treated in two ways: either considered as normal HABs or ignored. If twin boundaries are considered, the grain size is less than 4 µm, and increases only slightly during recrystallization. If twin boundaries are ignored, the grain size increases with time but remains less than 10 µm even at the almost fully recrystallized state.

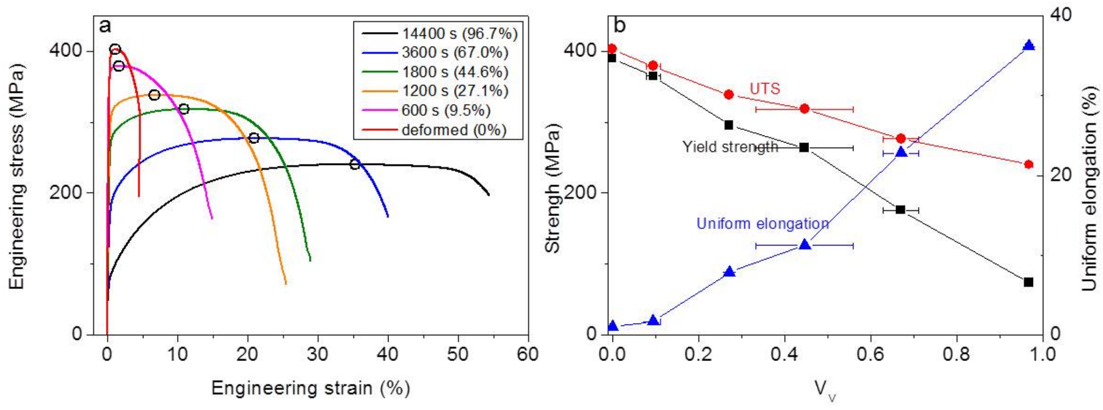

Fig. 4 Tensile properties of the as-deformed and partially recrystallized samples. a) Tensile curves with the uniform elongation e_u and ultimate tensile strength s_u marked by circles. b) Evolution of the yield strength s_y, s_u and e_u as a function of the recrystallized volume fraction V_V.

<u>3.3 Mechanical properties.</u> Fig. 4a shows that the cold-rolled sample has a high strength but the uniform elongation is very limited (1%), which is typical for heavily deformed metals. With increasing V_V, the uniform elongation increases gradually while the strength decreases. The yield strength s_y (0.2% offset), the ultimate tensile strength s_u and the uniform elongation e_u (elongation at maximum load) as a function of V_V are plotted in Fig. 4b. s_y, s_u decrease, while e_u

increases, roughly proportionally to V_V. However, some deviations from a linear relation are observed, e.g. e_u at small V_V.

4. MODELLING AND DISCUSSION

A way to model the dependence of the mechanical properties on V_V is to consider the partially recrystallized sample as a composite made of two phases: one recrystallized and the other deformed. In the applied model, it is assumed that deformation is uniform throughout the two phases:

1) The local strain tensor is uniform and equal to the macroscopically imposed strain tensor, i.e. $\boldsymbol{\varepsilon}_{rex} = \boldsymbol{\varepsilon}_{def} = \boldsymbol{\varepsilon}$
2) The deformed matrix is a homogeneous aggregate, and its strength is identical to that of the rolled sample. When loaded in uniaxial tension, the rolled sample necks soon after yielding. Therefore, we consider that work hardening is negligible and assume a constant flow stress (i.e. Fig. 5a):
$$\sigma_{def} = \sigma_{0,def} \tag{2}$$
3) The flow curve of the recrystallized volume is assumed to be identical to that of the fully recrystallized sample. In this work, the tensile true-stress true-strain curve of the sample annealed for 144000s (V_V=96.7%, referred as 'recrystallized' in the following) is used to represent the flow curve of the recrystallized part, and fitted by a Voce law (Voce 1948) (see Fig. 5a):
$$\sigma_{rex} = \sigma_{\infty,rex} - (\sigma_{\infty,rex} - \sigma_{0,rex})\exp(-\varepsilon_{rex}\Theta_{0,rex}/\sigma_{\infty,rex}) \tag{3}$$
4) The flow stress of the sample σ is obtained by volume averaging:
$$\sigma = V_V\sigma_{rex} + (1 - V_V)\sigma_{def} \tag{4}$$

This type of model is widely used for composite materials (Meyers and Chawla 2009), and has also been used for partially recrystallized materials (e.g. Hansen and Vandermeer 2005, Hong, Tao, Zhang, Huang and Lu 2014). Using this model, we may predict the flow stress of a partially recrystallized sample. The predicted flow curve for V_V=67% (corresponding to the sample annealed for 3600 s) is shown in Fig. 5a. Compared with the experimental flow curve, the predicted curve tends to slightly underestimate the flow stress.

The model also yields analytical expressions of s_y, s_u and e_u. The yield strength s_y is calculated as:

$$s_y = \sigma_y = V_V\sigma_{0,rex} + (1 - V_V)\sigma_{0,def} \tag{5}$$

The Considère criterion is applied to determine the onset of localized deformation:

$$\Theta_u = (d\sigma/d\varepsilon)_u = \sigma_u \tag{6}$$

where Θ_u and σ_u are, respectively, the work hardening rate and flow stress of the sample at the uniform strain. Using the four assumptions mentioned above, this criterion is written as:

$$V_V\Theta_{rex,u} = V_V\sigma_{rex,u} + (1 - V_V)\sigma_{0,def} \tag{7}$$

Since the flow stress of the recrystallized part is assumed to follow the Voce law (Eq. 3), the work hardening rate of the recrystallized part is expressed as:

$$\Theta_{rex} = \Theta_{0,rex}(1 - \sigma_{rex}/\sigma_{\infty,rex}) \tag{8}$$

By combining Eq. 7 and 8, the flow stress in the recrystallized part at uniform elongation can be obtained:

$$\sigma_{rex,u} = (\sigma_{\infty,rex}/(\Theta_{0,rex} + \sigma_{\infty,rex}))((V_V\Theta_{0,rex} - (1 - V_V)\sigma_{0,def})/V_V) \tag{9}$$

The stress of the whole sample at uniform strain, i.e. the uniform stress, then equals:

$$\sigma_u = V_V\sigma_{rex,u} + (1 - V_V)\sigma_{0,def} = \frac{\Theta_{0,rex}}{\Theta_{0,rex}+\sigma_{\infty,rex}}(V_V\sigma_{\infty,rex} + (1 - V_V)\sigma_{0,def}) \tag{10}$$

Since the uniform stress must not be less than the yield stress, Eq. 10 only applies when V_V is larger than a critical value. This critical V_V is obtained by setting Eq.10 equal to Eq. 5:

$$V_{V,cr} = \frac{\sigma_{\infty,rex}\sigma_{0,def}}{\Theta_{0,rex}(\sigma_{\infty,rex}-\sigma_{0,rex})+\sigma_{\infty,rex}(\sigma_{0,def}-\sigma_{0,rex})} \tag{11}$$

In general, the uniform stress is

$$\sigma_u = \begin{cases} \frac{\Theta_{0,rex}}{\Theta_{0,rex}+\sigma_{\infty,rex}}(V_V\sigma_{\infty,rex} + (1 - V_V)\sigma_{0,def}) & V_V > V_{V,cr} \\ V_V\sigma_{0,rex} + (1 - V_V)\,\sigma_{0,def} & V_V \le V_{V,cr} \end{cases} \tag{12}$$

The corresponding uniform strain ε_u can be deduced using Eq. 3 and 9 for $V_V > V_{V,cr}$, while for $V_V \le V_{V,cri}$, $\varepsilon_u = 0$.

The e_u and the s_u are calculated by converting the ε_u and σ_u to enigeering strain/stress:

$$e_u = \exp(\varepsilon_u) - 1 \tag{13}$$

$$s_u = \frac{\sigma_u}{1+e_u} = \frac{\sigma_u}{\exp(\varepsilon_u)} \tag{14}$$

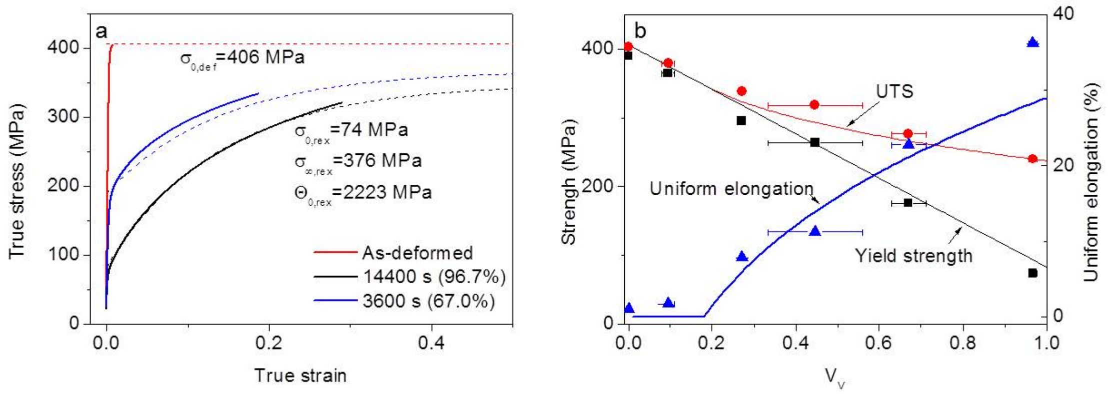

Fig. 5 Modelling and experimental results for the tensile properties. a) The solid lines show the experimental flow curves converted from the engineering curves (Fig. 4a). The parts after uniform elongation are not shown. The dashed lines in red and in black are curves used to represent the flow curves of the deformed and recrystallized parts, respectively, and the values of the fitting parameters are listed. The dashed line in blue is the predicted flow curve for V_V=67%, corresponding to the sample annealed for 3600 s. b) The predicted s_y, s_u and e_u as a function of V_V. The experimental results from Fig. 4b are shown as points.

The calculated s_y, s_u and e_u from the analytical solutions are plotted in Fig. 5b, which agrees relatively well with the experimental results. Two features of the partially recrystallized microstructure are important here. First, the isostrain assumption is usually considered as an upper-bound approximation of the response of polycrystals. It works best for two types of composites: 1) composites with unidirectionally aligned continuous fibres loaded along the fibre direction (e.g. Mileiko 1969), 2) laminated composites loaded parallel to the laminate plane (e.g. Semiatin and Piehler 1979). In this work, the recrystallized grains cluster in bands parallel to

RD, and the loading direction is also parallel to RD, which makes the partially recrystallized sample analogous to a laminate composite. Second, the grain size (intercept length including twin boundaries) increases only slightly during recrystallization (see Fig. 3b), and this change of grain size has negligible effects on the flow curves. Therefore, it is considered acceptable to use the flow curve of the recrystallized sample (annealed at 230 °C for 14400 s Vv=96.7%) to represent that of the recrystallized grains also in the partially recrystallized sample.

However, there are two major discrepancies between the prediction and the experimental results: 1) the uniform elongation for the sample annealed for 14400 s is underestimated (see Fig. 5b); 2) the predicted flow curves (see Fig. 5a) and also s_u (see Fig. 5b) are slightly lower than the experimental ones. The first discrepancy is partly due to the selection of the Voce law in order to fit the flow curve of the recrystallized sample. The Voce law predicts a constantly decreasing work hardening rate (with strain and stress), and does not consider a constant work hardening rate occurring at later stages of plastic deformation (Kocks and Mecking 2003). It can be seen from Fig. 5a that the fitted curve for the recrystallized sample is lower than the experimental one for strains >0.2. A better prediction of the uniform elongation may be obtained using a better work hardening law (e.g. Pantleon 2005) or using directly the experimental flow curve (losing the opportunity of analytical solutions). The second discrepancy may be related to two factors. First, the deformed matrix does have some work hardening ability, which is not included in the modelling. Second, the strain may not be uniformly distributed: the recrystallized grains or at least part of the recrystallized grains may deform more than the external strain, and thus be work hardened more. Both factors may increase the predicted flow stress of the partially recrystallized sample. The partitioning of strain during tensile tests is an important issue in plasticity modelling. It depends on various factors, including the difference of flow stresses of the deformed/recrystallized volume, and the spatial distribution of the recrystallized grains. In-situ tensile tests combined with EBSD may provide useful information in this respect, which is the topic of on-going work. Furthermore, it should be noted that recovery of the unrecrystallized matrix is not considered in this model, which may affect the flow curve of the deformed part. More experimental works (e.g. microhardness, differential scanning calorimetry) are needed to estimate the extent of the recovery.

5. CONCLUSIONS

Microstructures and mechanical properties of a series of partially recrystallized copper samples were investigated. After partial recrystallization, recrystallized grains are clustered along bands parallel to the rolling direction. An analytical model is suggested to explain the observed mechanical properties of the partially recrystallized samples, in which it is suggested that the samples can be considered as a laminated composite. The model further assumes isostrain conditions. It is found that the predicted yield strength, ultimate tensile strength, and uniform elongation agree reasonably well with the experimental results for samples with recrystallization fractions covering the range from 0%-80%. The differences between the modelling and experimental results are evaluated, and strain partitioning between recrystallized and unrecrystallized parts is among the important factors, which may be verified by in-situ tensile experiments in the near future.

ACKNOWLEDGEMENTS

FXL wishes to thank Dr. N. Hansen and Dr. C.S. Hong for helpful discussions. FXL, YBZ and DJJ gratefully acknowledge the support from the Danish National Research Foundation (Grant No. DNRF86-5) and the National Natural Science Foundation of China (Grant No.

50911130230) for the Danish-Chinese Center for Nanometals, within which this work was performed. LD is mandated by the Belgian National Fund for Scientific Research (FNRS).

REFERENCES

Avrami, M. (1939). Kinetics of phase change. I. J. Chem. Phys. 7, 1103-1112.

Hansen N. and Vandermeer R.A. (2005) Recovery, recrystallization, and grain growth. In. Encyclopedia of condensed matter physics. Eds. F. Bassani, J. Liedl, P. Wyder, Elsevier, 5, 116-124.

Hong C.S., Tao N.R., Zhang Y., Huang X. and Lu K. (2014) Estimation of tensile uniform elongation of partially recrystallized Cu-Al alloy based on the rule of mixtures. These proceedings.

Jin H. and Lloyd D.J. (2004). Effect of a duplex grain size on the tensile ductility of an ultra-fine grained Al-Mg alloy, AA5754, produced by asymmetric rolling and annealing. Scr. Mater. 50, 1319-1323.

Johnson W.A. and Mehl R.F. (1939). Reaction kinetics in processes of nucleation and growth. Trans. AIME 135, 416-458.

Kocks U.F. and Mecking H. (2003). Physics and phenomenology of strain hardening: the FCC case. 48, 171-273.

Kolmogorov A.N. (1937). On the static theory of metal crystallization. Izv. Akad. Nauk. USS-Ser-Matermat. 1, 355-360.

Li Y.S., Zhang Y., Tao N.R. and Lu K. (2008). Effect of thermal annealing on mechanical properties of a nanostructured copper prepared by means of dynamic plastic deformation. Scr. Mater. 59, 475-478.

Lin F.X., Pantleon W., Leffers T. and Juul Jensen D. (2012). Effects of initial parameters on the development of cube texture during recrystallization of copper. Mater. Sci. Forum 702-703, 398-401.

Lin F.X., Zhang Y.B., Tao N.R., Pantleon W., Juul Jensen D. (2014). Effects of heterogeneity on recrystallization kinetics of nanocrystalline copper prepared by dynamic plastic deformation. Acta Mater. 72, 252-261.

Meyers M.A. and Chawla K.K. (2009). Mechanical behavior of materials. Cambridge University Press, 780-785.

Mileiko S.T. (1969). The tensile strength and ductility of continuous fibre composites. J. Mater. Sci. 4, 974-977.

Pantleon W. (2005). Disorientations in dislocation structures. Mater. Sci. Eng. A 400-401, 118-124.

Ray R.K., Hutchinson B. and Ghosh C. (2011). ‘Back-annealing’ of cold rolled steels through recovery and/or partial recrystallization. Inter. Mater. Rev. 56, 73-97.

Ridha A.A. and Hutchinson W.B. (1982). Recrystallization mechanisms and the origin of cube texture in copper. Acta Metal. 30, 1929-1393.

Semiatin S.L. and Piehler H.R. (1979) Deformation of sandwich sheet materials in uniaxial tension. Metal. Trans. A 10, 85-96.

Voce E. (1948) The relationship between stress and strain for homogeneous deformation. J. Inst. Metals 74, 537-562.

Wagner P., Engler O. and Lücke K. (1995). Formation of Cu-type shear bands and their influence on deformation and texture of rolled fcc {112}<111> single crystals. Acta Metall. Mater. 43, 3799-3812.

Wu G.L. and Juul Jensen D. (2008). Automatic determination of recrystallization parameters based on EBSD mapping. Mater. Charact. 59, 794-800.